# A HAMR Media Technology Roadmap to an Areal Density of 4 Tb/in$^2$

Dieter Weller[1], Gregory Parker[1], Oleksandr Mosendz[1], Eric Champion[2], Barry Stipe[1], Xiaobin Wang[3,4], Timothy Klemmer[5], Ganping Ju[5], and Antony Ajan[2]

[1]HGST a Western Digital company, San Jose Research Center, San Jose, CA 95135 USA
[2]Western Digital Corporation, Longmont, CO 80504 USA
[3]Seagate Technology, Bloomington, MN USA
[4]Avalanche Technology, Fremont, 94538 USA
[5]Seagate Technology, Fremont, CA 94538 USA

**This paper discusses heat-assisted magnetic recording (HAMR) media requirements and challenges for areal densities (AD) beyond 1 Tb/in$^2$. Based on recent roadmap discussions the focus is primarily on granular chemically ordered $L1_0$ FePtX-Y-perpendicular media with reduced average grain size down to $\langle D \rangle = 3$-5 nm relative to current CoCrPt based perpendicular magnetic recording (PMR) media with average grain size $\langle D \rangle = 7$-9 nm. In HAMR media the combination of thermal conductivity and Curie temperature $T_C$ determines the required laser power during recording. Key challenges are sigma variations of D and $T_C$ which need to be reduced to $\sigma_D/D \sim 10$-15% and $\sigma_{TC}/T_C \sim 2\%$. In addition AD is limited by switching field distribution (SFD) and thermal spot size. The key goal going forward is to optimize heads, media, head-media-spacing (HMS) and read-back channel technologies to extend AD to 4 Tb/in$^2$ and beyond.**

***Index Terms*—Anisotropy, Curie temperature, FePt media, grain size, heat-assisted magnetic recording.**

## I. Introduction

NOISE performance and spatial resolution are key parameters in magnetic recording media and are ongoing challenges to advance the areal density (AD). The dominant media noise source today is transition jitter. In sputtered media, it reflects the finite size, random positioning and dispersion in size, orientation and magnetic properties of the fine grains that comprise the media. Highly anisotropic materials, combined with heat-assisted magnetic recording (HAMR), promise significant reductions in the average, thermally stable grain size from currently 7–9 nm in CoCrPt to 3-5 nm in chemically ordered $L1_0$ FePt-based media [1]. $AD = 1 +$ Tb/in$^2$ has been demonstrated by Seagate in 2012 (see A.Q. Wu *et al.* [2]). Modeling results and requirements going forward have been discussed by X. Wang *et al.* [3]. TDK has reported an AD of 1.5 Tb/in$^2$ [4]. The bit-aspect ratio (BAR) in the TDK case was 1.2, significantly lower than in the Seagate demonstration. The current Advanced Storage Technology Consortium (ASTC) roadmap [1]–[3] proposes a BAR in the range 5 down to 3, when increasing AD from 1 up to 4 Tb/in$^2$.

HAMR media requirements based on modeling are highlighted in Table I based on ASTC discussions [1]. Besides grain size, shape and distribution, thermal properties of both magnetic and seed layers need to be optimized to achieve proper signal-to-noise ratio (SNR) for higher areal density. The data in Table I reflect an update of the recently published work by X. Wang *et al.* [3], where 6.4 nm bit length (4000 kfci) and 35 nm track width (725 ktpi) leading to $AD = \mathrm{kfci} \times \mathrm{ktpi} = 2.9$ Tb/in$^2$ with BAR $\sim 5.5$ were assumed. Optical near-field transducer (NFT) Peg heads together with thermal and micro-magnetic properties as well as HAMR extendibility and limitations are discussed in references [2] and [3]. Specific technology challenges include switching field distributions (SFD) at elevated temperature, saturation noise and NFT thermal spot size limits [5]. Elevated temperature refers to $\sim$ 20-50 K below the Curie temperature during cooling and where recording, i.e. aligning the bit direction up or down, takes place.

TABLE I
Proposed HAMR Media AD Requirements at 2 and 4 Tb/in$^2$ Based on Recent Modeling Discussion [1] and Publication [3]

| Areal Density (Tb/in$^2$) | 2 | 4 |
|---|---|---|
| KTPI | 700 | 1155 |
| KBPI | 2800 | 3464 |
| BAR | 4 | 3 |
| thermal gradient @ writing (K/nm) | 14 | 18 |
| $D_p$ center to center (nm) | 7.0 | 5.1 |
| D core (nm) | 6.0 | 4.3 |
| σ / mean grain diameter | 0.1-0.15 | 0.1-0.15 |
| $M_S$ film (emu/cm$^3$) (300 K) | 700 | 800 |
| $M_S$ core (emu/cm$^3$) | 875 | 1000 |
| $K_u$ (erg/cm$^3$) (300 K) | 3.50E+07 | 5.00E+07 |
| $H_K$ (kOe) (300 K) | 80 | 100 |
| $\sigma_{HK}/H_K$ (%) | 5.0-10.0 | 5.0-10.0 |
| $T_C$ (K) | <=750 | 700 - 750 |
| $\sigma_{Tc}/T_C$ (%) | 2.0 | 2.0 |
| $\sigma_\theta$ (deg) | 2.0 | 0.8 |
| media thickness (nm) | 9 | 8.2 |
| thickness / grain size ratio | 1.29 | 1.60 |
| SUL requirement | yes | yes |
| jitter (nm) | 1.55 | 1.43 |
| jitter / bit length (%) | 17.1 | 19.5 |
| grains / bit | 6.7 | 6.2 |
| grains / read width | 4.0 | 3.7 |

Manuscript received May 29, 2013; revised July 22, 2013; accepted August 30, 2013. Date of publication September 06, 2013; date of current version December 23, 2013. Corresponding author: D. Weller (e-mail: Dieter.Weller@HGST.com).

Color versions of one or more of the figures in this paper are available online at http://ieeexplore.ieee.org.

Digital Object Identifier 10.1109/TMAG.2013.2281027

The main focus today is to optimize high magnetic anisotropy thermally stable grains in well textured and chemically ordered $L1_0$ FePtX-Y based media. Compositions include $X = Ag$, Cu, Ni… and $Y = C$, $SiO_2$, $TiO_2$ [6]–[12] as is discussed in detail in this roadmap paper. Requirements and designs strongly depend on the type of recording heads, the spacing between heads and media (HMS) and the head-disk interface (HDI) [13]. The average grain pitch (core size) in the Seagate $1 +$ Tb/in$^2$ AD demonstration is 10.5 nm (9 nm) [2], [3]. It needs to be reduced down to 7 nm (6 nm) at 2 Tb/in$^2$ and down to 5.3 nm (4.3 nm) at 4 Tb/in$^2$. The relative grain size distribution $\sigma_D/D$ needs to be reduced at least down to 10-15%. Soft underlayers (SUL) are needed to optimize the write field orientation and sharpen the transitions. Magnetization density, thickness and reduced HMS optimize the read-back signal.

The current HAMR recording density is limited by the switching field distribution (SFD) and thermal spot size [2], [3]. The grain pitch was $D_p = 10.5$ nm at 1 Tb/in$^2$ [2], [3] and needs to be significantly reduced down to $D_p \sim 5$ nm to reach AD $\sim$ 4Tb/in$^2$. The parameters in Table I are based on micromagnetic simulations up to 2.9 Tb/in$^2$ [3]. The criteria to achieve specific densities are simulated based on a track signal-to-noise ratio above 10 dB and a track width smaller or equal to the corresponding TPI requirement. The 4 Tb/in$^2$ requirements were scaled based on the up to 2.9 Tb/in$^2$ AD simulations [1], [3].

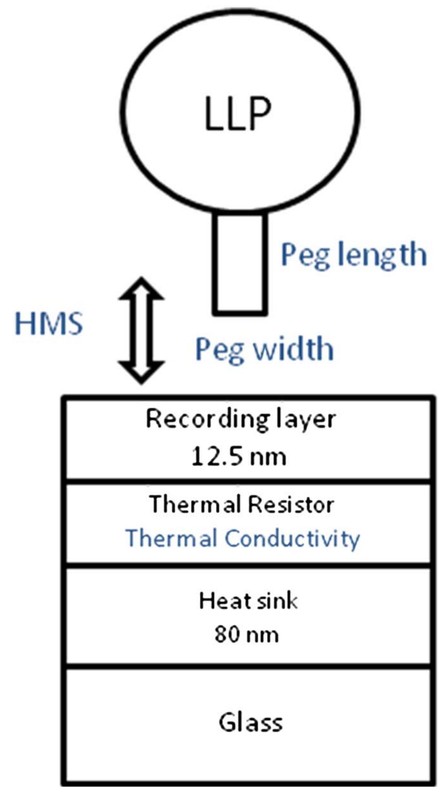


Fig. 1 Head and media description by Wang et al. [3]. Peg length and width for the LLP (lollipop) NFT, HMS, anisotropy ratio and thermal conductivity are key parameters.

## II. HAMR Media Design

Fig. 1 shows the current head-media design emphasizing lollipop (LLG) Peg heads [13]. The micro-magnetic simulations at 2.9 Tb/in$^2$ emphasize $D_G = 4$ nm grain size, $H_K = 90$ kOe room temperature anisotropy field, 10 nm Peg width and 36 nm FWHM diameter thermal spot size [3].

The key HAMR media challenges going forward are listed in Table II, which highlights issues, possible solutions and important research projects. It also indicates manageable and high, but solvable risks. Key challenges are (1) Curie temperature distribution (2) grain size and shape control, (3) 3-5 nm grain diameter at high AD, (4) thermal design and control for AD $>$ 3 Tb/in$^2$, (5) grain morphology and (6) dc noise reduction. Other challenges, e.g. HMS and HDI have been discussed by B. Marchon *et al.* [13]. All these topics are highlighted in Table II and discussed in Sections II-A–II-F.

### A. Curie Temperature Distribution

Controlling $\sigma_{TC}$ and reducing $\sigma_D$ below 15% of small grains requires improved sputter conditions, optimized seed layers and growth temperatures as well as optimized exchange coupled continuous granular composite (CGC) and/or exchange coupled composite (ECC) type structures. Characterizing grain size and Curie temperature distributions is critical.

The correlation between media $T_C$ and recording power needs modeling and experiments. Lowering $T_C$ by 100-150 K from 750 K to 650-600 K by adding $\sim$ 10 at% Ni or Cu is beneficial as it reduces the heat power requirement [14], [15]. Metrology and correlation of $\sigma_{TC}$ with $\sigma_D$ is critical, because they depend on each other. Reducing $\sigma_{TC}/T_C$ down to 2% based on roadmap requirements is likely very demanding. Therefore, optimizing sputter conditions, seed layers and growth temperature and perhaps using ECC, CGC or ECC + CGC combination type structures such as FePt/Fe [16] or FePt/FeRh [17], included in modeling [18] may help.

Fig. 2 shows the $T_C$ dependence on grain size and chemical ordering based on publications in 2006 [19], [20] (experiments), 2008 [21] (experiments and modeling) and more recently in 2012 [22], [23] (modeling). The smaller the grains, the more difficult it will be to achieve $\sigma_{TC}/T_C = 2\%$. Appropriate metrology to measure $\sigma_{TC}$ is needed to make progress.

Quantitative correlations show that the long-range chemical ordering parameter S, the Curie temperature $T_C$, and also the saturation magnetization $M_S$ drop about 10-20%, when decreasing particle or grain size (S vs D and $T_C$ vs D) as shown in Fig. 2 [19]–[21]. Direct evidence for grain size-dependent chemical and magnetic ordering in $L1_0$-FePt nanoparticles was obtained by measuring monodisperse nanoparticles prepared by a "salt-matrix annealing" technique (see Rong *et al.* [19]). Recent modeling efforts by O. Hovorka *et al.* (2012) [22] and A. Lyberatos *et al.* (2012) [23] confirm these results.

To measure $\sigma_{TC}$, accurate magnetization versus temperature measurements and likely new tools allowing relatively fast M (T) measurements up to $T_C$ are needed. Results as shown in Fig. 2 will help to estimate $\sigma_{TC}$ and come up with approaches to lower it down to 2%, based on the currently proposed roadmap requirements (Table I). Note that a distribution in $T_C$ may result in a smeared $H_K$ (T) dependence and thus reduce $dH_K/dT$ near

TABLE II
HIGH RISK HAMR MEDIA CHALLENGES, KEY ISSUES, POSSIBLE SOLUTIONS AND IMPORTANT RESEARCH PROJECTS [1]. BASED ON THE ASTC HAMR MEDIA DISCUSSION, AT AD = 2 Tb/in$^2$ RISK MITIGATION OF ALL THE MEDIA CHALLENGES REQUIRES SUSTAINED AND SYSTEMATIC DEVELOPMENT. AT AD = 4 Tb/in$^2$ ALL REQUIREMENTS LISTED IN Table I ARE VERY RISKY BUT NOT IMPOSSIBLE TO ACHIEVE

| MEDIA CHALLENGES | KEY ISSUES | POSSIBLE SOLUTIONS | IMPORTANT RESEARCH PROJECTS |
|---|---|---|---|
| Curie temperature distribution | low $\sigma_{Tc}$/Tc ~ 2% requirement | improved sputter conditions, seed layers, growth temperature and optimized exchange coupling | new characterization techniques, correlation of $\sigma_{Tc}$/Tc with grain size distribution |
| grain size and shape control | grain size fluctuations causing Curie temperature distributions, effective writeability and bit definition | improved seedlayers, optimized deposition conditions, propergrain segregants | alternative FePt texture layers |
| 3-5 nm grains at high areal density | increased switching field and grain size distributions | controlled and improved strain and surface anisotropy | density functional and atomistic calculations of the effect of increasing surface/volume ratio on Tc and Ku |
| thermal design and control for AD>3Tb/in$^2$ | effective thermal gradient and delivery of energy to FePt, achieving sufficient SNR | using high thermal conductivity heat sinks (HS) and/or plasmonic underlayers (PUL) | thermal-electomagnetic multiphysics modeling of near field transducers (NFT) and plasmonic underlayers (PUL) |
| grain morphology | control of the mean and distribution of grain size and thickness/diameter aspect ratio, columnarity, grain boundary width and roughness | improved segregants, alloys, alloy stacks, well textured underlayers, optimized growth rate etc. | FePtX-Y with new alloy components X and segregants Y, multiple layer structures and new seed layers with proper (200) orientation |
| dc noise reduction | rapid thermal cooling leading to incomplete magnetization reversal, dc noise affecting high data rate | optimize high data rate (short cooling time), single and multiple layers and thicker media with proper texture and orientation | DC noise model based on Tc and grain size distributions |

$T_C$. This will result in a lower effective write field gradient and additional noise. Hence low $\sigma_{TC}$ values of the order of 2% or better are necessary to achieve higher HAMR areal densities.

Ultimately one needs to optimize the thermal HAMR media properties, which influence heating and cooling rates! Anisotropy field dispersions need to be extended from PMR [24] to HAMR and will require new high field and temperature dependent magnetization tools as discussed by Ganping Ju [25].

### B. Grain Shape and Size Control

Variation in grain size and shape, which leads to distributions in $T_C$ and writeability and ultimately bit definition, are key issues. Possible solutions include new and improved seedlayers as well as optimized sputter conditions and appropriate segregants. In particular, finding alternative seed and texture layers beyond MgO is important.

Fig. 3 shows FePtAg-C results, which highlight a grain size sigma of $\sigma_D = 16\%$ at an average grain size of $\langle D \rangle = 7.2$ nm [26]. These granular media were deposited at 500-550°C on a 10 nm thick MgO seed and texture layer. As highlighted by O. Mosendz *et al.* [26] and L. Zang *et al.* [27], [28], Carbon segregated grains are rather spherical and not cylindrical. Also there are roughness effects and thermally unstable grains smaller than $D \sim 3$ nm are usually formed (see Fig. 3b).

The National Institute of Materials Science (NIMS) in Japan highlights the microstructure of $L1_0$ FePtX-Y, which involves glass substrates / heat sink layers / conductive interlayers and growth at elevated temperature of 450°C [26]. Seedlayer texture, orientation and size as well as shape of the grains (cylinders vs spheres) strongly depend on the segregants [27], [28]. Using $Y = C$ generally results in spherical grains [25]–[29] and $Y = SiO_2, TiO_2$ [30], [31] results predominantly in cylindrical grains.

Based on discussions it makes sense to investigate new segregants, use double instead of single magnetic layers and optimize seed layers with "perfect" (001) texture [30]. In $FePt\text{-}SiO_2$ granular films, the phase separation tendency is weak and it does not form completely decoupled granular structures [30], [31]. $FePt\text{-}TiO_2$ granular films develop better columnar structure with small grain size, but the perpendicular coercivity is "lost" due to suppression of $L1_0$ chemical ordering and therefore magnetic anisotropy by dissolution of Ti into FePt [30]. Granular films with mixtures of $C + SiO_2$ and $C + TiO_2$ show improved microstructure, but the combination of granular structure and hard magnetic properties fails [30]. Controlling the phase separation driving force appears to be one of the key requirements to achieve an "ideal" microstructure in FePtX-Y media..

The combination of FePtX-Y double layers, e.g. $Y_1 = C$ and $Y_2 = SiO_2$ or $TiO_2$ including an adhesion layer (100 nm

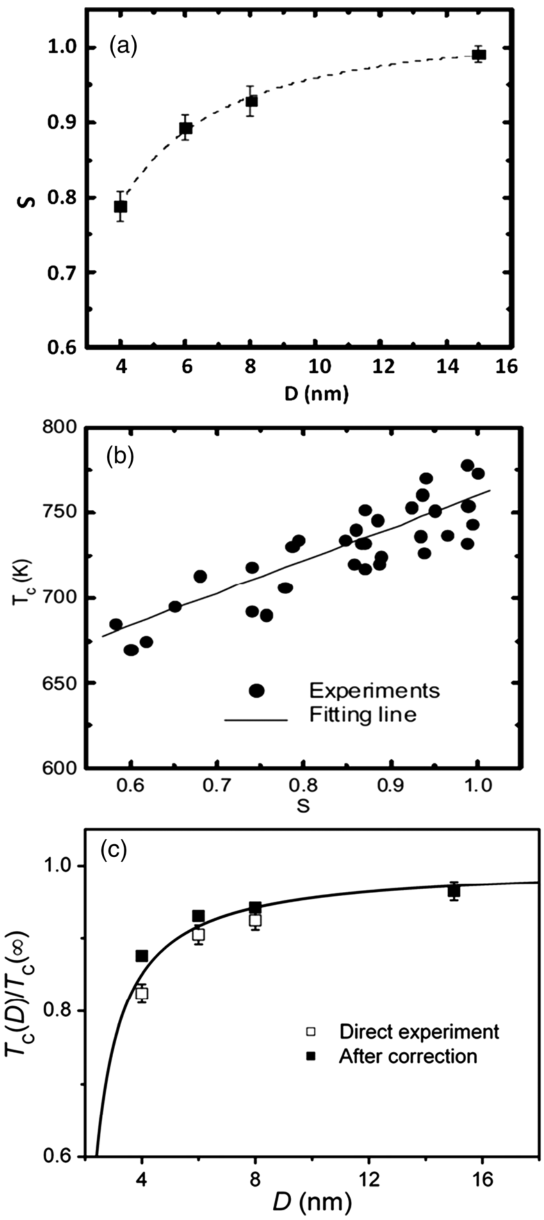


Fig. 2 (a) Chemical ordering parameter S vs grain size D and (b) Curie temperature $\mathrm{T_C}$ vs S of $\mathrm{L1_0}$ FePt magnetic nanoparticles from C.-B. Rong et al. (2006) [19], [20]; (c) $\mathrm{T_C}$ vs D from H. M. Lu et al. (2008) [21]. After J. P. Liu and H. M. Lu with their permission.

NiTa) and a seed layer (10 nm MgO) are summarized in Fig. 4 and Table III, which show that there are pros and cons [30].

Going forward it will be important to measure grain compositions, e.g. the radial and vertical Pt/Fe ratio with high resolution scanning tunneling microscopy (STEM) and electron energy loss spectroscopy (EELS) / energy dispersive X-ray spectroscopy (EDX) [32]. Measuring such localized grain compositions as a function of grain size is important to understand noise sources. Experimental and theoretical investigations e.g. of CoPt nanoparticles show size dependent compositions depending on the growth temperature [33]. Similar effects will likely occur in FePt grains [32].

Current MgO seed layers need to be improved (lattice constants, thickness, thermal conductivity etc) to optimize the

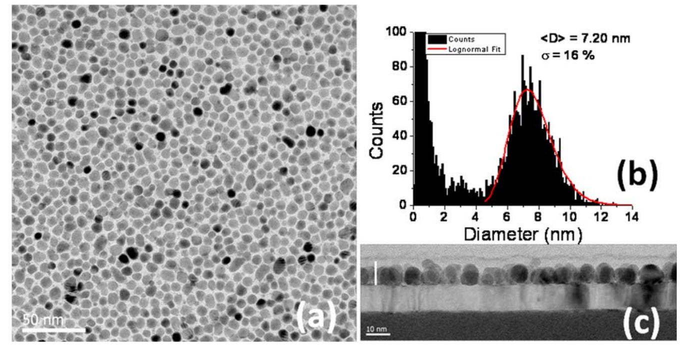


Fig. 3 (Color online) (a) Plan view TEM image showing granular FePtAg-C media. (b) Histogram of the grain size distribution. The red line is a lognormal fit resulting in $\langle \mathrm{D} \rangle = 7.2$ nm and low $\sigma_\mathrm{D}/\mathrm{D} = 16\%$. (c) The cross-sectional TEM image shows spherical grain shapes [26].

FePtX (002) grain orientation and to control heatflow into the heatsinks (e.g. Ag, Au, Al, Cu, Cr) and adhesion layers (e.g. NiTa). Grain homogeneity is very critical. Ultimately, the write-head optical power capability will determine thermal property requirements for the media. The effort remains to reduce the grain size and optimize shape and size distributions with less amounts of segregants ($< 40$ vol%) (see Section II-E and Fig. 6).

### C. Less Than 5 nm Grain Size at High AD

Reducing grain size and switching field distributions will be challenging. Possible solutions include control of strain and surface anisotropy. Also density functional and atomistic calculations of the effect of surface / volume ratio on $\mathrm{T_C}$ and $\mathrm{K_u}$ and respective experiments are important.

Achieving average grain size $\langle \mathrm{D} \rangle \leq 5$ nm, $\sigma_\mathrm{D}/\langle \mathrm{D} \rangle \leq 15\%$, columnar structure, smooth surfaces, good grain separation and high texture is very challenging. When the average grain size decreases, one has to expect $\mathrm{T_C}$ to decrease [19]–[23]. This will naturally lead to a wider variation of the Curie temperature due to the grain size distribution. This larger Curie temperature distribution $\sigma_{\mathrm{Tc}}/\mathrm{T_C}$ will result in larger DC noise and jitter. Furthermore, reduction of grain size may also lead to a larger distribution of the chemical ordering parameter S, thereby resulting in not only an additional contribution of the Curie temperature but also a wider distribution of the intrinsic $\mathrm{H_K}$, which further increases media noise. Finally, as the grain size decreases, stochastic thermal fields will increase, which can also increase media noise.

One approach to overcome these increasing distributions is to increase the thermal gradient in the recording layer. From a thermal design point of view achieving thermal gradients in excess of 15-20 K/nm is extremely difficult. What we have projected is in the 15-16 K/nm range for 3-4 Tb/in$^2$. While there may be a maximum at higher gradients it is not clear how to get there from the thermal design point of view. Another approach is to narrow the grain size and chemical ordering parameter, S, distributions. This will relax the requirement of high thermal gradients. However, due to the smaller grain values, the increased stochastic thermal fields will still cause additional noise (both DC and jitter). One obvious way to overcome this is by increasing the write field magnitude to insure that the Zeeman energy can

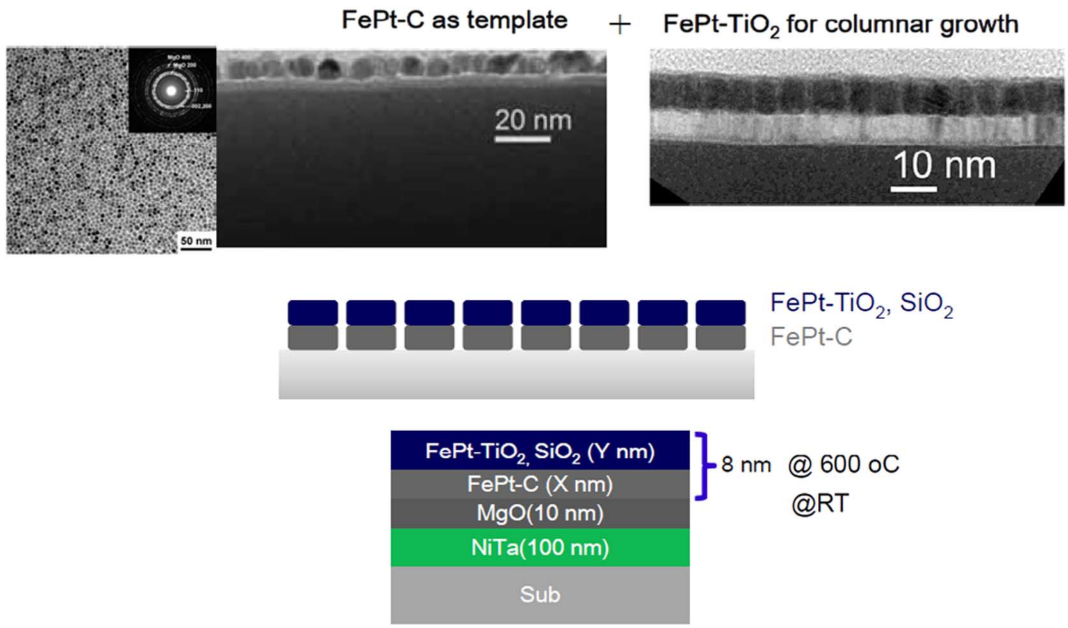


Fig. 4 Combination of FePt-C and FePt-TiO$_2$, SiO$_2$ double layers After K. Hono (NIMS) with his permission.

TABLE III
(BELOW): $Y_1 = C$ VS $Y_2 = SiO_2$ OR $TiO_2$ BASED ON REF. [30]. AFTER K. HONO (NIMS) WITH HIS PERMISSION

| C segregant (40 vol%) | $SiO_2$ or $TiO_2$ segregants (50 vol%) |
|---|---|
| 1. Good particle separation | 1. Poor particle separation |
| 2. High degree of $L1_0$ ordering | 2. Poor degree of $L1_0$ ordering |
| 3. Spherical type grains | 3. Cylindrical type grains |
| 4. Rough surface | 4. Excellent surface smoothness |

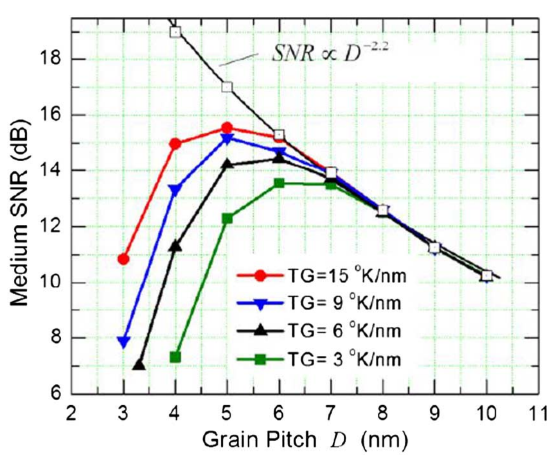


Fig. 5 Calculated SNR vs grain pitch D. For each data point, the recording field amplitude is optimized for maximum SNR. The open squares reflect SNR without thermal agitation for recording with thermal gradient TG = 15 K/nm. The read track width is fixed at W = 30 nm. Model assumptions include $H_K$ = 60 kOe, $M_S$ = 750 emu/cc, t = 10 nm, $\sigma_{HK}$ = 10%, $\sigma_{Tc}$ = 0% and $dH_K/dT \sim 600$ Oe/K. After Jimmy Zhu et al. [34] with his permission.

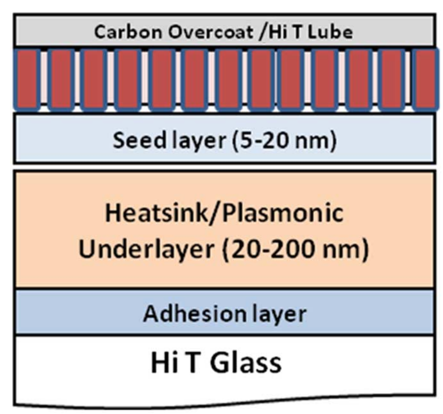


Fig. 6 Basic HAMR media design including granular FeXPt-Y alloys separated by segregants Y. Seed layers like MgO or alternatives establish proper FePt(002) texture. Heatsinks / plasmonic underlayers like Ag, Au, Al, Cu, Cr in combination with NiAl adhesion layers establish proper thermal gradients and optimize write power requirements. Future HAMR media design goals include $\langle D \rangle \sim 4$ nm, $\sigma_D \sim$ 10-15% and $\sigma_{TC} \sim 2\%$.

properly align the magnetic moment in the desired direction. Since the variance of the stochastic field varies inversely with the volume of the grain, this would imply the field magnitude would need to increase inversely as the square root of the grain volume.

As indicated in Table I, ultimately small grains (down to $D = 4$ nm) and small dispersions (toward $\sigma_D < 15\%$) are needed. Jimmy Zhu discussed SNR vs grain pitch modeling depending on the thermal gradient (TG) [34]. His main conclusion is that a grain-pitch GP = 4-5 nm leads to the highest possible SNR. The thermal gradient needs to be as high as possible, e.g. $T_G = 15$ K/nm as shown in Fig. 5.

The correlation between thermal gradient (TG) and the highest medium SNR in Fig. 5 highlights an achievable SNR of 15-16 dB for a grain pitch GP = 5 nm and TG = 15 K/nm [33]. Increasing TG to 50 K/nm would result in a maximum SNR $\sim$ 17 dB at GP = 4 nm [35]. Key is that smaller grains need higher thermal gradients to achieve proper SNR results.

### *D. Thermal Design and Control for* AD $> 3$ *Tb/in*$^2$

Key issues are achieving high thermal gradients and efficient delivery of energy to the media. To achieve that, plasmonic underlayers (PUL) in combination with proper heatsink materials as well as microstructure improvements are worked on. Important research projects include thermal and electromagnetic multi-physics studies of near-field transducers (NFT) and PULs.

Considering the problem of increased media noise as the average grain size decreases, the thermal design of HAMR media needs to be explored in order to obtain sufficiently high thermal gradients. Optimizing the underlayers is an obvious path to control the thermal resistances and limit the direct heat flow through the recording layer. An additional approach is to introduce a plasmonic underlayer (PUL) like AgX into the media stack [5], [36]. This metallic layer would limit the lateral spread of the evanescent wave from the near-field transducer (NFT). Both theoretical and experimental work is needed to confirm and quantify the feasibility of this approach. Reducing $T_C$ helps to reduce the required laser power and thermal reliability but it degrades SNR, since the effective $H_K$ gradient is reduced, i.e. there is less temperature difference between $T_C$ and room temperature. Accordingly it becomes a reliability performance tradeoff that has to be optimized for the given system. From a thermal design point of view achieving a thermal gradient in excess of 15–20 K/nm is extremely difficult. What is projected is in the 16 K/nm range for 3–4 Tb/in$^2$. While there may be a maximum at higher gradients it is not clear how to get there.

### *E. Grain Morphology*

Sufficient control of mean grain size and distribution, improved grain aspect ratio (thickness / diameter), columnar growth, narrow grain boundary width and reduced media roughness are key requirements. New segregants, alloy additions / compositions, stacks of double layers etc, textured underlayers, optimized growth rate and sufficient chemical ordering are being worked on [27]–[30].

Besides $L1_0$ chemical ordering, which requires high temperature deposition in the range 450–650$^\circ$C one needs to achieve near perfect (002) orientation ($\Delta\theta < 3^\circ$) and a size distribution of 10-15% or lower. Seed layers like MgO (100) (or alternatives) and heatsink (thermal conductivity) layers are critical.

Many options have been explored since the early 90's to develop small grain granular chemically ordered $L1_0$ FePtX-Y based media [11], [37], [38]. Details listed below and respective references are published in reference [11].

Seed layers promoting $L1_0$ FePt (001) perpendicular orientation with (200) textured underlayers that have been studied, include Pt/Cr, CrRu, RuAl, TiN, Cr, CrMo, Ti, TiC, Ag and MgO. The current focus is 5–15 nm thick fcc MgO seedlayers with (200) orientation and 9% lattice mismatch with FePt.

Heatsink layers, which are critical to control the thermal conductivity during HAMR recording include Ag, Au, Al, Cu and Cr. NiTa is also used as an appropriate adhesion layer on glass.

FeXPt alloy additions to optimize/reduce the growth temperature and Curie temperature include Au, Ag, Ni and Cu. 5–10 at% Ag can be used to reduce the deposition / annealing temperature and Cu or Ni are used to reduce $T_C$.

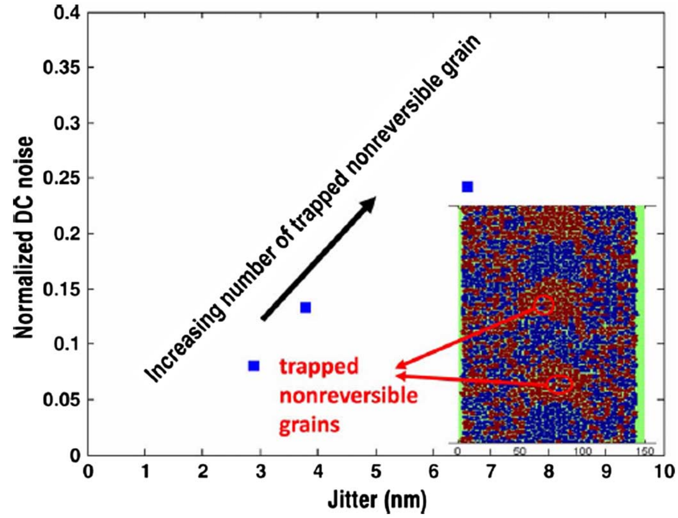


Fig. 7 DC-noise vs jitter based on X. Wang et al. (Seagate) [3] with their permission.

FePt-Y segregants are needed to decrease the grain size and exchange coupling. Many segregants have been tried including $SiO_2$ $TiO_2$, $AlO_x$, $Al_2O_3$, AlN, TaN, Ag, MgO, $Ta_2O_5$, W, Ti, $B_2O_3$, B/Ni, C/BN, $SiN_x$, $SiN_x/C$ and C.

Based on the Japanese National Institute for Materials Science (NIMS) [30], today's focus is on modified MgO seed layers, NiTa adhesion layers, and magnetic double layers with segregants $Y1 = 30–50$ at%C and $Y2 = 30–50$ at% $SiO_2$ or $TiO_2$.

### *F. DC Noise Reduction*

Fast thermal cooling leads to incomplete and insufficiently sharp bit edges. Possible solutions require exploration of high data rate (short cooling time), single and multiple media layers as well as thicker media with proper texture and orientation. Modeling dc-noise based on $T_C$ and grain size distributions is expected to make progress.

The dependence of ac/dc noise on media roughness and grain size distribution, $T_C$ distribution and thermal conductivity needs to be optimized. DC noise is due to un-switched grains and strongly depends on the recording speed. It is caused by stochastic processes during cooling and thus different grains will cause DC noise during repeat attempts. Typically, the faster the recording is the higher the DC noise will be. Detailed discussions can be found in reference. [3] The key is that recording with magnetization switching probability smaller than one causes dynamic switching variations which contribute to both dc-noise and jitter. Strong correlations of dc-noise and jitter from ref. [3] are shown in Fig. 7 for a range of switching probabilities. Normalized dc-noise in the figure is defined as signal standard deviation over signal mean value outside of the transition region.

A key path to reduce these dc noise issues is to optimize the thermal heating and cooling time (recording time) and use higher write fields. Media multilayer or ECC designs may also help to improve the media. The main conclusions are that performance of HAMR is characterized by measuring the transition jitter. The total jitter can be separated into two main components: jitter due to thermal randomness and jitter due to grain irregularity. Other jitter sources include field and thermal gradients as well as media switching field distributions. The simulation results suggest that jitter is reduced by intergranular exchange, nonzero canting angle of applied field, relatively large head field strength, maximum temperature of the heat spot about 100–150 K above the Curie temperature, and relatively low head velocity. These latter two results appear to stem directly from the physical inability to minimize both types of jitter simultaneously [39]. These results can be used for future optimizations in HAMR.

## III. Alternatives to FePt HAMR Media

In addition to the current focus on $\mathrm{L1_0}$-FePtX-Y, alternative high $\mathrm{K_u}$ materials may be considered. Details correlating anisotropy and minimum thermally stable grain size have been discussed several times [11], [40], [41]. Just from the anisotropy perspective, Rare Earth type materials, such as $\mathrm{SmCo_5}$ or $\mathrm{Fe_{14}Nd_2B}$ may be of interest. So far, they have not been considered, mostly because of corrosion issues. However, the recent announcement of Helium drives by HGST may relax this constraint and possibly make these viable alternative material sets to FePt. Of particular interest is $\mathrm{Nd_2Fe_{14}B}$, which has a lower $\mathrm{T_C}$ (585 K) than FePt (770 K) or $\mathrm{SmCo_5}$ (1000 K). Also the magnetic anisotropy is high enough to allow small grains down to $\mathrm{D} = 3.4$ nm also erase $\mathrm{D} = 2.1$ nm, as discussed in recent publications [42], [43]. The reason why $\mathrm{SmCo_5}$ is less attractive is that lowering $\mathrm{T_C}$ down to $\sim 600$ K will significantly reduce Ku, and increase D. The challenge in making $\mathrm{Nd_2Fe_{14}B}$ thin films is that it needs to be deposited at elevated temperatures higher than FePt and its unit cell contains 68 atoms and is much more complex than $\mathrm{L1_0}$ FePt [11].

## IV. Summary

The present HAMR media roadmap paper is based on Advanced Storage Technology Consortium (ASTC) discussions and reflects the current status of media requirements (Table I). Key challenges and research activities to make areal density progress are summarized in Table II. The media focus is on chemically ordered $\mathrm{L1_0}$ FePt type media. The currently demonstrated HAMR areal density of AD $\sim$ 1–1.5 Tb/in$^2$ is limited by near field transducer (NFT) heads switching field distribution and thermal spot size in the media. Noise performance and spatial resolution are key challenges to increase the AD beyond 1–1.5 Tb/in$^2$ to 4 Tb/in$^2$ or higher. Magnetic grain sizes, shapes, size distributions and thermal properties as well as seed layers need to be improved and optimized to achieve the required SNR. Most critical going forward are low $\sigma_{\mathrm{TC}}$, $\sigma_{\mathrm{HK}}$, $\sigma_{\mathrm{Hex}}$ distributions, full $\mathrm{L1_0}$ FePt chemical ordering and "perfect" texture as highlighted in the proposed roadmap (Table I). Magnetic and structural media properties need to be optimized. Proper seed layers like MgO (200) achieve chemically ordered and well textured $\mathrm{L1_0}$ FePt (002) media. Heatsink layers like Ag, Au, Al, Cu or Cr control the thermal conductivity and are used to optimize the thermal gradient during recording. Current alloy additions in FePtX-Y are $\mathrm{X} = \mathrm{Ag}$ ($\sim$ 5–10 at%) to enhance the $\mathrm{L1_0}$ chemical ordering at a growth temperature down to 600–650°C and $\mathrm{X} = \mathrm{Cu}$ or Ni ($\sim$ 10 at%) to reduce the Curie temperature by 100-150 K down to $\mathrm{T_C} = 650$–600 K, which lowers the recording power requirement. Segregants in FePtX-Y like $\mathrm{Y} = \mathrm{C}$, $\mathrm{SiO_2}$ or $\mathrm{TiO_2}$ ($\sim$ 30–40 vol%) are used to decrease the grain diameter, avoid exchange coupling and optimize magnetic properties, however, progress needs to be made. In addition exchange coupled ECC and / or CGC structures e.g. FePt/Fe [16] or FePt/FeRh [17] based on modeling [18] will likely make sense.

## References


[1] D. Weller, X. Wang, E. Champion, G. Parker, T. Klemmer, A. Ajan, G. Ju, and B. Stipe, ASTC HAMR Media roadmap summary report and presentation Sep. 20–12, 2012 [Online]. Available: http://www.idema.org

[2] A. Q. Wu, Y. Kubota, T. Klemmer, T. Rausch, C. Peng, Y. Peng, D. Karns, X. Zhu, Y. Ding, E. KC. Chang, Y. Zhao, H. Zhou, K. Gao, J.-U. Thiele, M. Seigler, G. Ju, and E. Gage, "HAMR areal density demonstration of 1+ TBPSI on spinstand," *IEEE Trans. Magn.*, vol. 49, p. 779, 2013.

[3] X. Wang, K. Gao, H. Zhou, A. Itagi, M. Seigler, and E. Gage, "HAMR recording limitations and extendibility," *IEEE Trans Magn.*, vol. 49, p. 686, 2013.

[4] T. Nezu, TDK Claims HDD Areal Density Record Oct. 2, 2012, 14:37, Nikkei Electronics [Online]. Available: http://techon.nikkeibp.co.jp/english/NEWS_EN/20121002/243229

[5] W. A. Challener, C. Peng, A. V. Itagi, D. Karns, W. Peng, Y. Peng, XM. Yang, X. Zhu, N. J. Gokemeijer, Y.-T. Hsia, G. Ju, R. E. Rottmayer, M. A. Seigler, and E. C. Gage, "Heat-assisted magnetic recording by a near-field transducer with efficient optical energy transfer," *Nat. Photon.*, vol. 3, p. 220, 2009.

[6] L. Zhang, Y. K. Takahashi, A. Perumal, and K. Hono, "$\mathrm{L1_0}$-ordered high coercivity (FePt)Ag—C granular thin films for perpendicular recording," *J. Magn. Magn. Mater*, vol. 322, p. 2658, 2010.

[7] L. Zhang, Y. K. Takahashi, K. Hono, B. C. Stipe, J.-Y. Juang, and M. Grobis, "$\mathrm{L1_0}$-ordered FePtAg—C granular thin film for thermally assisted magnetic recording media," *J. Appl. Phys*, vol. 109, p. 07B703, 2011.

[8] O. Mosendz, S. Pisana, J. W. Reiner, B. Stipe, and D. Weller, "Ultra-high coercivity small-grain FePt media for thermally assisted recording," *J. Appl. Phys.*, vol. 111, p. 07B729, 2012.

[9] S. Pisana, O. Mosendz, G. J. Parker, J. W. Reiner, T. S. Santos, A. T. McCallum, H. J. Richter, and D. Weller, "Effects of grain microstructure on magnetic properties in FePtAg-C media for temperature assisted recording," *J. Appl. Phys*, vol. 113, p. 043910, 2013.

[10] B. H. D. Ch. S. Varaprasad, M. Chen, Y. K. Takahashi, and K. Hono, "$\mathrm{L1_0}$ ordered FePt based perpendicular recording media for heat assisted magnetic recording heat assisted magnetic recording," *IEEE Trans. Magn.*, vol. 49, p. 718, 2013.

[11] D. Weller, O. Mosendz, G. Parker, S. Pisana, and T. S. Santos, "$\mathrm{L1_0}$ FePtX-Y media for heat assisted magnetic recording," *Phys. Stat. Solid. A*, vol. 210, p. 1245, 2013.

[12] S. Wicht, V. Neu, L. Schultz, B. Rellinghaus, D. Weller, O. Mosendz, G. Parker, and S. Pisana, "Atomic resolution structure–property relation in highly anisotropic granular FePt-C films with near-Stoner-Wohlfarth behaviour," *J. Appl. Phys.*, vol. 114, p. 063906, 2013.

[13] B. Marchon, T. Pitchford, Y.-T. Hsia, and S. Gangopadhyay, "The head-disk interface roadmap to an areal density of 4 Tb/in$^2$," *Adv. Tribol.*, vol. 2013, 2013, article ID 521086.

[14] J.-U. Thiele, K. R. Coffey, M. F. Toney, J. A. Hedstrom, and A. J. Kellock, "Temperature dependent magnetic properties of highly chemically ordered Fe Ni Pt $\mathrm{L1_0}$ films," *J. Appl. Phys.*, vol. 91, p. 6595, 2002.

[15] B. Wang and K. Barmak, "Re-evaluation of the impact of ternary additions of Ni and Cu on the A1 to $\mathrm{L1_0}$ transformation in FePt films," *J. Appl. Phys*, vol. 109, p. 123916, 2011.

[16] B. Ma, H. Wang, H. Zhao, C. Sun, R. Acharya, and J.-P. Wang, "Structural and magnetic properties of a core-shell type $\mathrm{L1_0}$ FePt/Fe exchange coupled nanocomposite with tilted easy axis," *J. Appl. Phys.*, vol. 109, p. 083907, 2011.

[17] J.-U. Thiele, S. Maat, and E. E. Fullerton, "FeRh/FePt exchange spring films for thermally assisted magnetic recording," *Appl. Phys. Lett.*, vol. 82, p. 2859, 2003.

[18] D. Suess, J. Lee, J. Fidler, and T. Schrefl, "Exchange-coupled perpendicular media," *J. Magn. Magn. Mater.*, vol. 321, p. 545, 2009.

[19] C.-B. Rong, D. Li, V. Nandwana, N. Poudyal, Y. Ding, Z. L. Wang, H. Zeng, and J. P. Liu, "Size-dependent chemical and magnetic ordering in $L1_0$-FePt nanoparticles," *Adv. Mat.*, vol. 18, no. 22, p. 2984, 2006.

[20] J. Lyubina, B. Rellinghaus, G. Gutfleisch, and M. Albrecht, , K. H. J. Buschow, Ed., "Handbook of magnetic materials," in *Chapter 5, Structure and Magnetic Properties of* $L1_0$*-Ordered Fe-Pt Alloys and Nanoparticles*. New York: Elsevier, 2011.

[21] H. M. Lu, Z. H. Cao, C. L. Zhao, P. Y. Li, and X. K. Meng, "Size dependent ordering and Curie temperatures of FePt nanoparticles," *J. Appl. Phys.*, vol. 103, p. 123526, 2008.

[22] O. Hovorka, S. Devos, Q. Coopman, W. J. Fan, C. J. Aas, R. F. L. Evans, X. Chen, G. Ju, and R. W. Chantrell, "The Curie temperature distribution of FePt granular magnetic recording media," *Appl. Phys. Lett.*, vol. 101, p. 052406, 2012.

[23] A. Lyberatos, D. Weller, G. Parker, and B. C. Stipe, "Size dependence of the Curie temperature of $L1_0$-FePt nanoparticles," *J. Appl. Phys.*, vol. 112, p. 113915, 2012.

[24] G. Ju, H. Zhou, R. Chantrell, B. Lu, and D. Weller, "Direct probe of anisotropy field dispersion in perpendicular media," *J. Appl. Phys.*, vol. 99, p. 083902, 2006.

[25] G. Ju, "Metrology discussion," presented at the ASTC meeting, Jan. 2012.

[26] O. Mosendz, S. Pisana, J. W. Reiner, B. Stipe, and D. Weller, "Ultra-high coercivity small-grain FePt media for thermally assisted recording," *J. Appl. Phys.*, vol. 111, p. 07B729, 2012.

[27] L. Zhang, Y. K. Takahashi, A. Perumal, and K. Hono, "$L1_0$-ordered high coercivity (FePt)Ag—C granular thin films for perpendicular recording," *J. Magn. Magn. Mater.*, vol. 322, p. 2658, 2010.

[28] L. Zhang, Y. K. Takahashi, K. Hono, B. C. Stipe, J.-Y. Juang, and M. Grobis, "$L1_0$-ordered FePtAg—C granular thin film for thermally assisted magnetic recording media," *J. Appl. Phys.*, vol. 109, p. 07B703, 2011.

[29] S. Pisana, O. Mosendz, G. J. Parker, J. W. Reiner, T. S. Santos, A. T. McCallum, H. J. Richter, and D. Weller, "Effects of grain microstructure on magnetic properties in FePtAg-C media for temperature assisted recording," *J. Appl. Phys.*, vol. 113, p. 043910, 2013.

[30] B. S. D. Ch. S. Varaprasad, M. Chen, Y. K. Takahashi, and K. Hono, "$L1_0$ ordered FePt based perpendicular recording media for heat assisted magnetic recording heat assisted magnetic recording," *IEEE Trans. Magn.*, vol. 49, p. 718, 2013.

[31] E. Yang and D. E. Laughlin, "$L1_0$ FePt-oxide columnar perpendicular media with high coercivity and small grain size," *J. Appl. Phys.*, vol. 104, p. 023904, 2008.

[32] S. Wicht, V. Neu, L. Schultz, O. Mosendz, S. Pisana, D. Weller, and B. Rellinghaus, "Atomic resolution TEM study of FePt heat-assisted magnetic recording media," *J. Appl. Phys.*, to be published.

[33] D. Alloyeau, G. Prevot, Y. Le Bouar, T. Oikawa, C. Langlois, A. Loiseau, and C. Ricolleau, "Ostwald ripening in nanoalloys: When thermodynamics drives a size-dependent particle composition," *Phys. Rev. Lett.*, vol. 105, p. 255901, 2010.

[34] J.-G. (Jimmy) Zhu and H. Li, "Understanding signal and noise dependences in heat assisted magnetic recording," *IEEE Trans. Magn.*, vol. 49, p. 765, 2013.

[35] J.-G. (Jimmy) Zhu, in *DSSC Meeting CMU-Pittsburgh October 2012 and most recent May 13, 2013 DSSC Meeting in Mountain View, CA*.

[36] J. A. Schuller, E. S. Barnard, W. Cai, Y. C. Jun, J. S. White, and M. L. Brongersma, "Plasmonics for extreme light concentration and manipulation," *Nature Mat.*, vol. 9, pp. 193–204, 2010.

[37] S. D. Granz and M. H. Kryder, "Granular $L1_0$ FePt (001) thin films for heat assisted magnetic recording," *J. Magn. Magn. Mater.*, vol. 324, p. 287, 2012.

[38] Y. Peng, J.-U. Thiele, G. Ju, T. P. Nolan, Y. Ding, and A. Q. Wu, "Recording layer for heat assisted magnetic recording," US Patent 2013/0004796 A1, Jan. 3, 2013.

[39] R. H. Victora and P.-W. Huang, "Simulation of heat assisted magnetic recording using renormalized media cells," *IEEE Trans Magn.*, vol. 49, p. 751, 2013.

[40] D. Weller and A. Moser, "High Ku materials approach to 100 Gb/in$^2$," *IEEE Trans. Magn.*, vol. 35, p. 4423, 1999.

[41] D. Weller and T. McDaniel, "Advanced magnetic nanostructures," in *Media For Extremely High Density Recording*. New York: Springer, 2007, ch. 11.

[42] T. Sato, H. Kato, T. Shima, Y. K. Takahashi, and K. Hono, "Effect of film morphology on the magnetic properties for Nd–Fe–B thin films," *J. Magn. Magn. Mater.*, vol. 323, p. 163, 2011.

[43] J. F. Herbst, J. J. Croat, and F. E. Pinkerton, "Relationships between crystal structure and magnetic properties in $Nd_2Fe_{14}B$," *Phys. Rev. B*, vol. 29, p. 4176, 1984.